Available online at www.sciencedirect.com

SCIENCE DIRECT®

C. R. Physique 4 (2003) 675–685

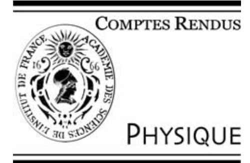

Semiconductor lasers/Lasers semiconducteurs

InP-based wavelength tunable vertical cavity surface emitting laser structures

Isabelle Sagnes [a], Martin Strassner [e,1], Sophie Bouchoule [a,*], Jean-Louis Leclerq [b], Philippe Regreny [b], Aldrice Bakouboula [c], Frank Riemenschneider [d], Peter Meissner [d]

[a] *Laboratoire de photonique et nanostructures, LPN, CNRS UPR 20, route de Nozay, Marcoussis, France*
[b] *CRELYMO, LEOM, CNRS UMR5512, École centrale de Lyon, Ecully, France*
[c] *CRELYMO, LPM, UMR CNRS 5511, INSA de Lyon, Villeurbanne, France*
[d] *Technical University Darmstadt, Darmstadt, Germany*
[e] *Institute for Microelectronics and Information Technology, Kungl Tekniska Högskolan – KTH, Stockholm, Sweden*

Received 21 February 2003; accepted 26 February 2003

Presented by Guy Laval

Abstract

We report on the design, fabrication and characteristics of both hybrid and monolithic micro-electro-mechanically wavelength tunable 1.55 μm InP-based Vertical-Cavity Surface-Emitting Laser (VCSEL) structures. Photo-pumped tunable VCSELs are successfully realized using both configurations, and a design for electrically pumped tunable VCSEL is presented. ***To cite this article: I. Sagnes et al., C. R. Physique 4 (2003).***
© 2003 Académie des sciences. Published by Éditions scientifiques et médicales Elsevier SAS. All rights reserved.

Résumé

Structures laser à cavité verticale à base d'InP accordables en longueur d'onde. Nous présentons la conception, la fabrication et les caractéristiques de lasers à cavité verticale accordables en longueur d'onde mettant en œuvre une configuration hybride et une configuration en intégration monolithique. Dans les deux cas l'émission laser accordable en longueur d'onde a été obtenue en régime de pompage optique. Un concept de laser monolithique accordable pompé électriquement est également présenté. ***Pour citer cet article : I. Sagnes et al., C. R. Physique 4 (2003).***
© 2003 Académie des sciences. Published by Éditions scientifiques et médicales Elsevier SAS. All rights reserved.

Keywords: Tunable lasers; Vertical surface emitting lasers; III-V semiconductors; Micro-opto-electro-mechanical systems

Mots-clés : Lasers accordables ; Lasers à cavité verticale ; Semiconducteurs III-V ; Membranes semiconductrices

1. Introduction

During the last decades Vertical-Cavity Surface-Emitting Lasers (VCSELs) have generated a huge scientific interest. Among the advantages of VCSELs are wafer level fabrication and characterization, easy fiber coupling, and potentially low manufacturing costs. VCSELs are Fabry–Pérot (F–P) type lasers that are intrinsically single-mode and present a very high

* Corresponding author.
E-mail address: sophie.bouchoule@lpn.cnrs.fr (S. Bouchoule).

[1] Presently with laboratoire de photonique et nanostructures – LPN.

1631-0705/$ – see front matter © 2003 Académie des sciences. Published by Éditions scientifiques et médicales Elsevier SAS. All rights reserved.
doi:10.1016/S1631-0705(03)00082-3

mode selectivity, due to the very short cavity length and large longitudinal mode spacing. Moreover, the small active volume of a VCSEL enables it to operate at sub-mA laser threshold currents [1–3].

These benefits led to their successful introduction and commercial exploitation in the 850 nm and 980 nm wavelength range [4–7]. The short wavelength VCSELs rely on GaAs-based materials providing for highly reflective distributed Bragg reflectors (DBRs), active layer design, and current confining schemes. The implementation of wavelength division multiplex (WDM) systems based on optical fibers enforced the search for cheap and reliable lasers at longer wavelengths, i.e., 1.55 μm. However 1.55 μm VCSELs are more difficult to realize than their 0.85–0.98 μm counterparts. Indeed, while the InP material system is the best choice for active materials with high gain, such as InGaAs(P) or InGa(Al)As multi-quantum wells (MQWs), the available refractive index step within the family of lattice matched materials is considerably smaller than that available in the GaAs system. As a consequence, highly reflective DBRs can be realized only at the expense of a rather large number of quarter-wavelength (1/4-λ) pairs. Moreover, the rather poor thermal conductivity of quaternary layers lattice matched to InP, as compared to that of the binary GaAs/AlAs, is another drawback to achieve high laser performance. However, tremendous progress has been made during the past decade and efficient monolithic InP-based 1.55 μm VCSELs have been demonstrated, first in pulsed operation [8–11] then in continuous pumping regime [12–16].

As the number of channels in WDM systems is steadily increasing, the search for tunable light sources has been consolidated. Wavelength tunable devices are highly desirable sources to be used as spare and back-up components for fixed wavelength devices, and they are key elements in future all-optical switching and wavelength dynamic routing systems. In addition to the inherent advantages of the VCSEL structure already mentioned at the beginning, the possibility to tune the F–P laser mode continuously over more than 30 nm without any mode hopping due to the very large free spectral range of the VCSEL cavity as compared to currently deployed in-plane devices is particularly interesting. Since the pioneering work of some research groups [17,18] various monolithic concepts of micro-electro-mechanically tunable VCSEL have been presented, achieving output powers of up to 2 mW and tuning ranges of as much as 50 nm [19–22]. A more complete overview of their development can be found in [23].

In this paper, we will present a review of our work on both hybrid and monolithic micro-electro-mechanically tunable 1.55 μm InP-based VCSEL structures. Section 2 is dedicated to a brief review of VCSEL basics and some of the fundamental principles for wavelength tuning in VCSEL structures. Three different approaches to realize wavelength tunable devices are then presented: a hybrid approach based on a photo-pumped half-VCSEL structure assembled with a highly reflective GaAs-based membrane forming a long cavity VCSEL is presented in Section 3. The concept of a monolithic optically pumped InP-based tunable VCSEL using InP/air-gap DBRs is also discussed (Section 4) followed by the presentation of a design and first results for an electrically pumped tunable VCSEL relying on a tunnel junction for efficient carrier injection and an InP/air-gap top DBR that provides for the tuning (Section 5).

2. VCSEL basics and methods for wavelength tuning

As depicted in Fig. 1, the first obvious feature of a vertical cavity laser is that, in contrast to in-plane lasers, the cavity as well as the out-coupling direction of the optical beam are perpendicular to the wafer surface.

The second feature is that the length of the F–P cavity itself is much shorter than in a conventional laser, typically a few microns, that is of the same order as the wavelength. This results in a very high mode selectivity and longitudinal single-mode emission, but also in a much shorter gain region, which in turns leads to a much smaller round-trip cavity gain. As a consequence, the cavity mirrors have to be highly reflective (>99%), in order to compensate for the cavity losses, including the mirror losses. Such high reflectivity values can be obtained if one uses DBRs consisting of a high number of 1/4-λ pairs alternating two materials of low and high refractive index. The detailed theory of Bragg mirrors used in VCSEL structures is beyond the scope of this paper, and is presented in many books and references [1–3,24].

Let us recall some of the most important characteristics of such mirrors: first, the reflectivity of a DBR increases with the number of 1/4-λ pairs. However, due to the internal optical loss existing in the used materials, the reflectivity will saturate at

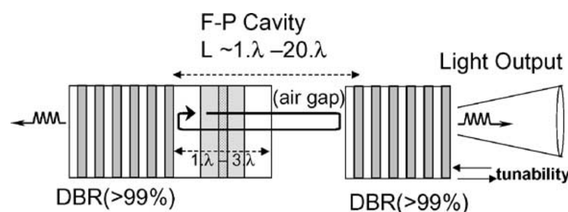

Fig. 1. Tunable VCSEL schematics.

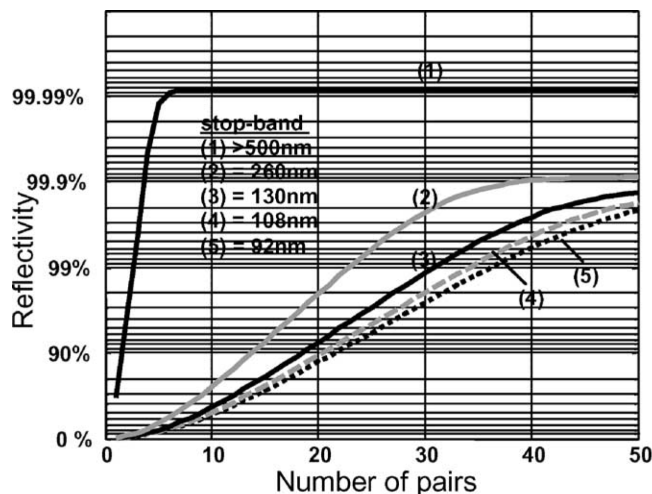

Fig. 2. Calculated reflectivity values at the Bragg wavelength as a function of the number of pairs in the Bragg mirrors. (1): InP/air, (2): GaAs/$Al_{85\%}$GaAs, (3): InP/InGaAlAs, (4): InAlAs/InGaAlAs, (5): InP/InGaAsP. Gap wavelength of the quaternary alloys is 1.43 µm.

a maximum value (<100%), depending on the average amount of optical losses. Finally, the high reflectivity value is obtained over a rather wide wavelength range around the Bragg wavelength, called the stop-band of the Bragg mirrors. The width of the stop-band directly depends on the refractive index step available between the high refractive index – and low refractive index – materials. These features are illustrated in Fig. 2, where several semiconductor materials are considered to realize a Bragg mirror at a center wavelength of 1.55 µm.

As can be seen, semiconductor InP-based mirrors such as InGaAsP/InP mirrors [8] or InAlAs/InGaAlAs mirrors [9] need a large number of pairs (>40) to achieve a reflectivity higher than 99%, which is only possible due to the very low optical losses in these materials. On the other hand, GaAs/AlAs-based mirrors need a lower number of pairs to achieve high reflectivity due to their higher index step, and the DBR stop-band is also enlarged. The great advantage of InP-based semiconductor mirrors over GaAs/AlAs mirrors is to be compatible with the growth of the InP-based F–P cavity and active layer, in a single epitaxial step. For this reason, an original and specific InP/InGaAlAs DBR configuration with improved reflectivity and thermal conductivity has been developed [25], that was successfully applied in the realization of hybrid tunable VCSELs presented in Section 3.

Finally, a very high index step and consequently a very wide stop-band and very high reflectivity can be obtained with few InP/air-gap 1/4-λ pairs. Since such air-gap mirrors combine simultaneously the advantages of being lattice matched to InP substrate, presenting a high index step, and having low optical losses, they are very attractive candidates to realize InP-based VCSELs strutures [26]. However, the fabrication process of such mirrors is rather critical and needs a careful study, as is presented in Section 4.

First 1.55 µm InP-based VCSELs have been demonstrated using lattice-matched bulk quaternary as an active layer [8]. The subsequent use of InP-based quantum wells allowed one to significantly reduce the laser threshold of the 1.55 µm VCSELs. Different types of quantum wells (QWs) and barriers, and different QWs number have been used in VCSEL structures, mainly InGa(Al)As/InGaAlAs [14,15], and InGaAs(P)/InGaAsP QWs/barriers [12]. The introduction of strain in the quantum wells [13,16] and the use of strain-compensated multi-quantum wells [8] as active layer allows one to further decrease the laser threshold.

Both optical pumping and electrical pumping can be used in order to maintain the threshold carrier density in the semiconductor active material. While electrical pumping is obviously the preferred technique to realize compact, low-cost and reliable devices, optical pumping is used as well to obtain laser operation since it does not need a specific design for current injection and current confinement. Optically pumped tunable VCSEL structures are presented in Sections 3 and 4.

In case of electrical pumping, a p–i–n junction must be formed on both sides of the F–P cavity. One of the first approaches consisted in p-doping and n-doping the top and bottom mirror, respectively, and localizing current injection with ion implantation [1,9]. However, highly doped mirrors, especially p-doped mirrors, present higher optical losses than undoped mirrors, mainly due to free carrier absorption [1–3], which reduce the effective mirror reflectivity. Also p-doped mirrors often present rather high resistivity due to the lower mobility in p-doped materials. As a consequence, such VCSEL structures often suffer from high series resistance, which, in conjunction with poor thermal conductivity of the InP-based quaternary materials, can significantly degrade the laser performance. Different electrical pumping schemes have been developed to overcome these difficulties. The most promising technique relies on a $n/n^{++}/p^{++}/p$ tunnel junction between one mirror and the intrinsic cavity

to enable current injection in the active layer. With this technique the two mirrors can be n-doped, or one mirror can be n-doped while the second is undoped, eliminating the inherent drawbacks of p-doped mirrors. Electrically pumped, monolithic, non-tunable VCSEL structures using this last configuration have been successfully fabricated and present to date among the best performances reported for single transverse-mode 1.55 μm VCSELs [16]. A similar structure adapted to the realization of wavelength tunable 1.55 μm VCSELs is presented in Section 5.

As depicted in Fig. 1, the basic principle used in this work to tune the emission wavelength of the VCSEL is to change the physical length of the F–P cavity. For this purpose an air-gap is included in the cavity, between the semiconductor part comprising the active layer, and the top mirror. By moving the top mirror back and forth, the air-gap thickness is varied, and consequently the overall cavity length is changed. In the case of micro-cavities of few wavelengths length that we consider here, a small movement of less than 1 μm of the top mirror corresponds to a continuous tuning of the F–P peak over several tens of nanometers. Such a technique enables in principle wavelength continuous tuning of the VCSEL over at least all the C-band of WDM systems (1530–1570 nm).

Several mechanisms have been studied to realize tunable micromechanical mirrors such as mirror deformation due to heating effect by current injection, or deflection due to electrosatic forces generated by an electrical field [23]. In this paper we present two types of tunable mirrors: the first type presented in Section 3 is a thermally actuated GaAs-based mirror. The second one described in Sections 4 and 5 is an InP/air-gap mirror that is tuned by applying an electrostatic force.

3. Hybrid tunable VCSEL

A micro-electro-mechanically tunable VCSEL based on a two-chip concept has been developed. It is composed of a bulk micromachined membrane chip holding a movable curved mirror membrane and a 'half-VCSEL' chip that consists of a solid bottom mirror and an amplifying active region. A similar concept has been previously used to fabricate tunable optical F–P filters showing excellent results [27,28].

The main advantage of the two-chip concept as compared to a monolithic solution is that both chips can be optimized separately. Furthermore, the two-chip approach allows easier implementation of a larger resonator length that should improve the linewidth of the lasers in a similar way that it reduces the transmission bandwidth of a F–P-filter. One of the drawbacks of this concept is the necessity for an additional assembly step to align both parts to each other increasing the production costs. A simple technique has been developed that allows attaching both chips together without any spacers and with a minimum of additional alignment steps [29].

Fig. 3 illustrates the two-chip concept of a photo-pumped VCSEL. The optical microcavity is formed by a fixed plane mirror (half-VCSEL chip 'B') and a movable curved mirror membrane that provides for the tuning (chip 'A'). When positioned against each other they define a stable plane-concave microcavity.

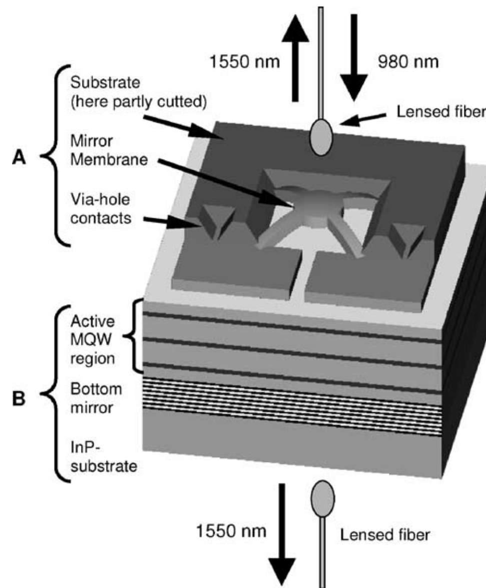

Fig. 3. Two-Chip Concept of an optically pumped VCSEL. A: membrane chip (upside down), B: 'half-VCSEL' chip.

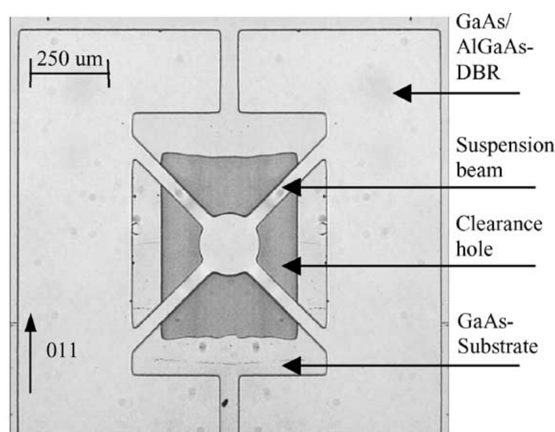

Fig. 4. Front view of a semiconductor membrane (chip A).

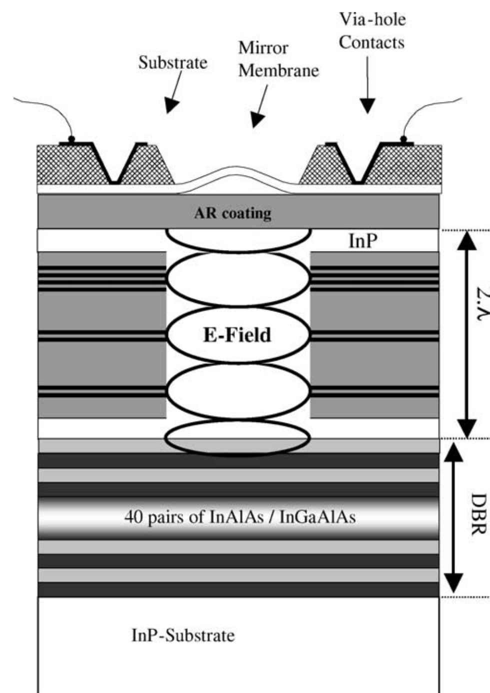

Fig. 5. Structure of the optically pumped 'half-VCSEL'. An anti-reflection (AR) coating is deposited on the top surface of the half-VCSEL chip to avoid parasitic intra-cavity reflections.

For the fabrication of the mirror membrane 19.5 periods $Al_{0.87}Ga_{0.13}As/GaAs$ and 5 periods $Al_{0.87}Ga_{0.13}A/In_{0.03}Ga_{0.97}As$ n-doped ($N_D \sim 5 \times 10^{17}$ cm^{-3}) 1/4-λ pairs were grown by MOVPE on top of a 500 nm thick AlGaAs etch-stop layer on an undoped GaAs-substrate. Such a DBR has a theoretical maximum reflectivity of 99.6% assuming an absorption coefficient of 10 cm^{-1}. The inclusion of 3% of Indium in the lower layers introduces an intrinsic stress component, leading to a concave bending of the membrane once the substrate is removed. By changing the length and width of the four suspension arms the radius of curvature (3–20 mm range) and the initial deflection of the membrane, i.e., the initial cavity length (up to 30 μm), can be adjusted. The curvature of the membrane is always rotation-symmetric as shown by white light interferometric measurements [28]. Additional deflection of the membrane is achieved by electro-thermal heating of the thin membrane's suspension arms. Via-hole contacts through the substrate are implemented to establish the electrical connections to the front of the membrane chip for this purpose.

The membrane geometry (arms, mirror diameter) is first defined by an etching step up to the GaAs substrate. After deposition of an adapted protection mask, a clearance hole is formed to release the membrane from the substrate. The detailed procedure for the membrane fabrication is presented elsewhere [27–29]. The front view of a semiconductor membrane is depicted in Fig. 4.

The structure of the semiconductor 'half-VCSEL' chip is composed of a 40-period lattice-matched InP-based bottom DBR centered at 1.6 μm, of a 2λ-thick active region capped by a top InP layer (Fig. 5). The active region has been designed to absorb the optical pump wavelength (980 nm) and consists of InGaAsP (λgap ∼ 1.2 μm, lattice matched to InP) cladding layers with three groups of unstrained InGaAs QWs and InGaAsP barriers (λgap ∼ 1.2 μm). The QWs are distributed on three successive anti-nodes of the standing wave in a periodic gain configuration [1] and the distribution starting from the top surface is 4–2–2 in order to uniformly excite the QWs by the optical pump. All these layers have been grown by MOCVD in a D125 EMCORE reactor on (001) InP-substrate

Once the cavity is assembled, the active region is pumped by injecting 980 nm CW laser light through a lensed fiber that produces a mode field diameter of 25 μm (see Fig. 3). The VCSEL output is measured at the backside of the InP-substrate using a second lensed fiber connected to an optical spectrum analyzer. The coupled output power of the VCSEL is reported as a function of incident 980 nm pump power in Fig. 6. Laser operation is achieved with a threshold of 30 mW (∼50 W/cm^2) incident power.

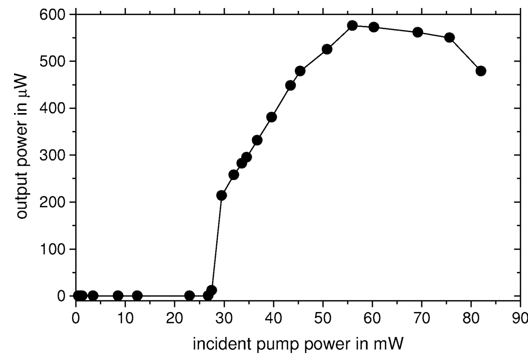

Fig. 6. Output power of the photo-pumped 1.55 µm VCSEL versus 980 nm pump power.

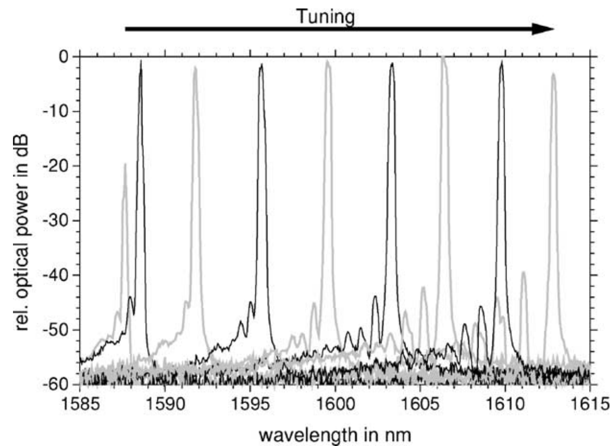

Fig. 7. Measured laser output spectrum during tuning.

Fig. 7 illustrates the tuning capability of the VCSEL: a tuning range of 24 nm in CW-operation at room temperature with approx. 0.5 mW output power is achieved by increasing the cavity length through displacement of the mirror membrane.

A novel two-chip concept for micro-mechanically tunable VCSELs has been presented and its feasibility concept has been confirmed by the fabrication and characterization of an optically pumped VCSEL. The presented concept is readily applicable to an electrically pumped VCSEL by simply replacing the optically pumped half-VCSEL chip with an electrically pumped version.

4. Two air gaps reflectors VCSEL

The second tunable VCSEL studied is a photo-pumped air-gap VCSEL relying on two micromechanical InP/air-gap DBRs forming the resonator. This device approach uses two semiconductor/air-gap DBRs to profit from the large difference in refractive index contrast leading to high reflectivity and reduced mirror losses. Another major advantage of these DBRs is the possibility to grow the entire epitaxial structure in a single run.

Fig. 8 shows the design of the tunable VCSEL. The top mirror consists of a p–i–n structure where the n-InP layer defining the upper part of the cavity is actuated electrostatically. An applied voltage causes this layer to move towards the thicker hence more rigid p-doped InP layer. Consequently the resonance of the VCSEL cavity will tune to longer wavelengths [30].

The F–P cavity is formed from a solid and an air-gap part. Two $\lambda/4$ air-gaps surround the solid part consisting of a periodic gain structure. Three packages of two strain compensated quantum wells are positioned at the anti-nodes of the optical standing-wave. They are embedded in InGaAsP ($\lambda_{gap} = 1.32$ µm) cladding layers to achieve a higher absorption of the pump light ($\lambda_p = 1.3$ µm). The optical thickness of the cavity's solid part is 2λ, giving an overall F–P cavity optical length of 2.5 λ. The bottom mirror is formed by a 4 period InP/air-gap DBR. Both InP/air-gap DBRs have a nominal reflectance of $>99.8\%$.

The fabrication procedure of the InP/air-gap mirrors, including the metal contacts definition on the n- and p-InP layers of the top InP-air gap DBR is detailed in [26,31]. Basically, InGaAs/InP stacks are epitaxially grown, and the InGaAs material

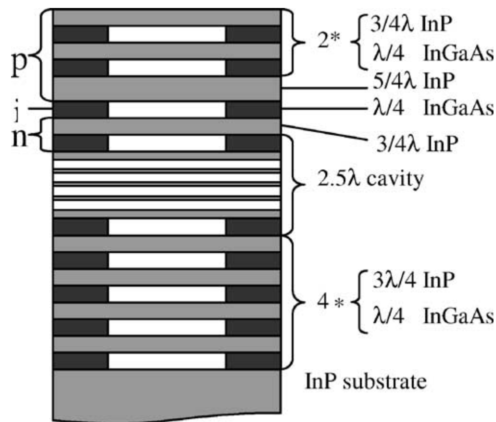

Fig. 8. Design of tunable VCSEL with two InP/air-gap mirrors.

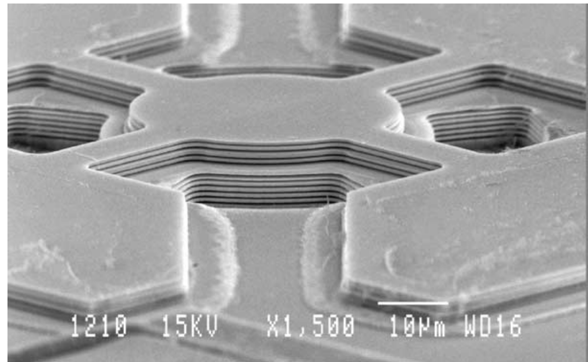

Fig. 9. SEM photograph of the processed photo-pumped VCSEL with two InP/air-gap mirrors.

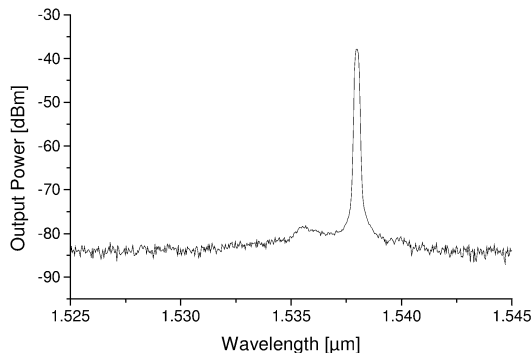

Fig. 10. VCSEL optical spectrum measured just above laser threshold.

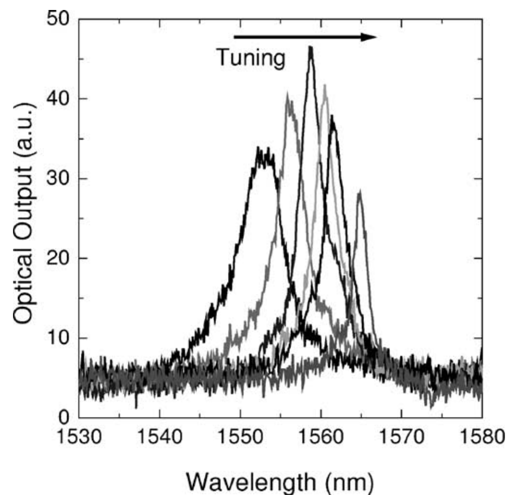

Fig. 11. Measured emission spectra of a resonant cavity device under tuning (bias voltage range is 20 V).

is then removed by selective chemical under-etching once the mirror geometry has been defined by a first dry etching step. Deformation of the released InP layers is a very important issue considering that the thickness of the layers is in the range of few quarter-waves and thus a small variation has a large effect on the optical properties of the final device. An arsenic carry-over process occurs during the MOVPE growth of the InGaAs/InP hetero-structure when growing InP after arsenic-containing materials like, e.g., InGaAs [32]. Since the resulting gradient distribution of arsenic in the InP layers induces stress and causes their deformation once they are released, it has to be minimized [33]. The processed photo-pumped VCSEL with two air-gap DBRs fabricated by surface micromachining of an InP/InGaAs epitaxial structure is shown in Fig. 9.

A cleaved single mode optical fiber (10 μm mode diameter) has been used to feed the pump radiation to the device and to collect the emitted light. The fiber has been positioned respective to the center of the device. The spectrum has been measured with an optical spectrum analyser.

Room temperature continuous wave lasing has been achieved. Fig. 10 shows a typical emission spectrum of the processed VCSELs just above threshold (4.2 mW pump power, i.e., around 50 $\mathrm{W/cm^2}$). The emission peak was at 1.54 μm and had a maximum output power of −35 dBm at room temperature (RT). The full width at half maximum (FWHM) of the emission peak is limited by the spectrum analyzer to 0.14 nm.

Due to the complex process the few devices found to be lasing were not tunable. Measuring on some of the non-lasing devices – working as tunable Resonant Cavity Light Emitting Diodes – the tuning characteristics have been obtained. Fig. 11

shows the emission spectrum of a RCLED under tuning. The emission wavelength has been shifted for 13 nm using a bias voltage of 20 V.

The low loss resonator provides for CW operation at room temperature, despite the poor thermal conductivity of air-gap reflectors. Moreover, the quaternary material which forms most of the active region has a poor thermal conductivity of only 5 W/mK as compared to 68 W/mK for InP. Using a simple analytical model we estimate a thermal resistance from the center of the pumped area to the supporting pads of approximately 35 °C/mW. The thermal resistance could be reduced by choosing a more favorable geometry (wider and shorter beams) or by increasing the thickness of the InP layers surrounding the active region. However, the aim of our design has been to demonstrate that a low loss, InP-based resonator can be fabricated and that lasing can be achieved with a low threshold. As our results indicate, internal heating is not critical for reaching the lasing threshold if a sufficiently high-Q resonator is used.

5. Monolithic tunable VCSEL with one air-gap mirror

The aim of our research effort is the fabrication of a micromechanical electrically tunable and electrically pumped VCSEL structure. In this last section the focus is thus on a monolithic solution which combines a top surface-micromachined InP/air-gap DBR monolithically integrated with an all-semiconductor half-VCSEL including an InP/InGaAlAs DBR. The cavity of the VCSEL forms a p–i–n junction comprising the MQWs active layer and an additional tunnel junction for the electrical pumping, which changes the design of the VCSEL significantly as compared to the photo-pumped VCSEL in Section 3.

As depicted in Fig. 12, the complete structure presents four electrical contact levels: the first one is formed on the backside of the n-doped InP substrate and connects the n-side of p–i–n junction through the n-doped DBR. A $n/n^{++}/p^{++}/p$ tunnel junction is integrated on top of the p-doped part of the junction and a second contact level through the p side of the junction is formed on the n-doped InP top layer. The third electrode contacts the p-doped layer of the air-gap DBR, while the fourth contact is deposited on the top of the n-doped upper region of the mirror, enabling electrical actuation and tunability towards longer wavelengths. An interesting feature of this new configuration is that the mirror could also be tuned towards shorter wavelength, by applying a voltage difference between the second and third contacts [34], the second (n-type) contact being a common contact for mirror and half-VCSEL chip.

One of the challenges is the epitaxial growth of a tunnel junction by MOVPE since it is difficult to obtain high doping level with an abrupt n^{++}/p^{++} interface in a rather thin region. So far, electrically pumped VCSELs using a tunnel junction for current injection have been grown by molecular beam epitaxy (MBE) [12,16,35].

The epitaxial structure consists of a 40 pairs InP/InGaAlAs Bragg mirror, and 8 InGaAs/InGaAlAs MQWs surrounded by two InGaAlAs undoped spacing layers. For the tunnel junction InGaAsP ($\lambda g \sim 1.4$ µm) quaternary alloy was chosen instead of InGaAlAs quaternary in order to be able to realize the highly doped p^{++}/n^{++} interface necessary for superior electrical characteristics. Since highly doped layers present increased optical losses, the p^{++}/n^{++} region forming the tunnel junction is as thin as possible (∼60 nm) limited by the MOVPE growth. Additionally, the highly doped layers are put at a node of the

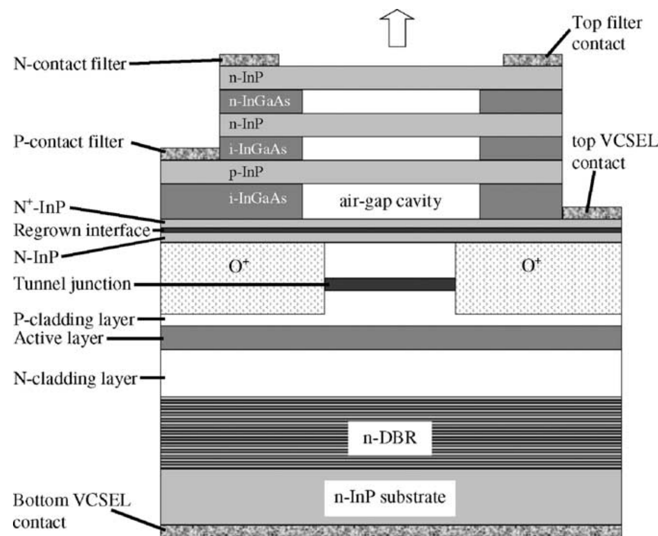

Fig. 12. Schematic diagram of the regrown tunable VCSEL for electrical pumping.

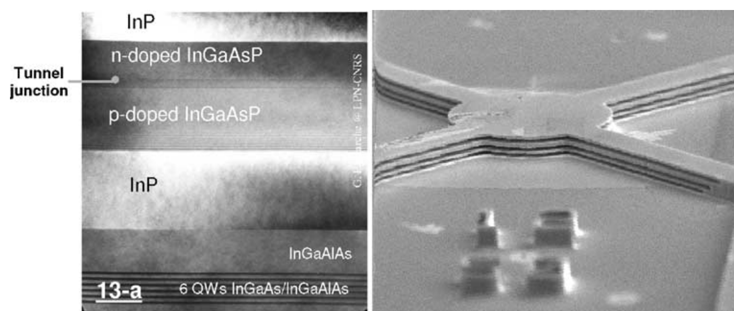

Fig. 13. TEM cross section view of the tunnel junction-based MOVPE structure (left), and SEM view of the SS-MBE regrown VCSEL (right).

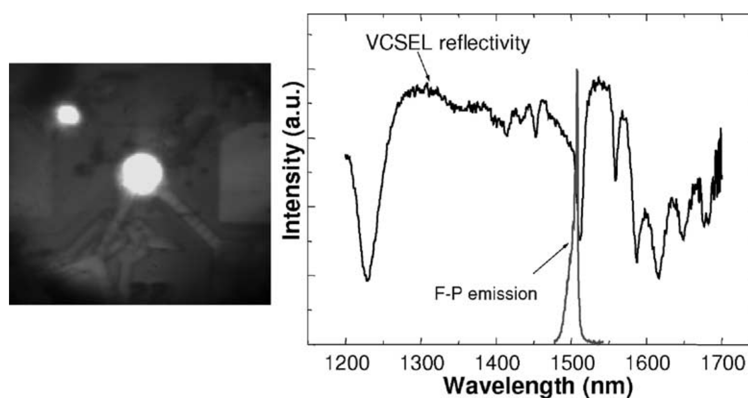

Fig. 14. Electro-luminescence image of the forward-biased half-VCSEL chip at ~ 1 kA/cm^2 (left), and Measured optical spectrum of the VCSEL under electrical injection. The measured reflectivity spectrum of the resonant cavity measured from the top of the InP/air-gap mirror is reported for comparison (right).

electrical field. The optical thickness of the entire semiconductor part of the F–P cavity corresponds to 3λ. Fig. 13(a) shows the high quality of the MOVPE growth.

Tunnel junction $n/n^{++}/p^{++}/p/n$ diodes have been preliminary processed to be compared with classical p–n junctions diodes. The current versus voltage curves of the diodes with InGaAsP tunnel junctions were exactly similar to those measured for the standard InP-based p–n junctions alone, proving the very good quasi-ohmic behavior of the tunnel junction. From diodes measurements with different diameters, we could estimate the average value of the specific resistance of the tunnel junction to be $5 \times 10^{-5}\ \Omega\cdot\text{cm}^2$.

The MOVPE growth of the all semiconductor bottom half-chip is followed by an O^{++} implantation step to localize the current injection in the active layer. The basic principle of this implantation step is to create mid-gap defects in the depth of the $n^{++}/p^{++}/p$ semiconductor layers and to locally reduce their conductivity [1]. In that way, the current injection in the active layer beneath the tunnel junction is limited to the non-implanted region. This approach was successfully applied for the realisation of monolithic nontunable 1.55 μm VCSEL [12].

A top InP/InGaAs stack is epitaxially regrown by Solid Source Molecular Beam Epitaxy (SS-MBE) taking advantage of the lower arsenic carry-over effect as compared to MOVPE. The structuring of the top mirror of the VCSEL is similar to the one of the two InP/air-gap VCSEL presented in Section 4. A detailed schematic of the completed monolithic tunable electrically-pumped VCSEL is shown in Fig. 12, and Fig. 13(b) shows a SEM photograph of the monolithically integrated InP/Air-gap mirror suspended above the all-semiconductor half-VCSEL chip.

Electroluminescence measurements performed at an injected current of 1 kA/cm^2 on the oxygen implanted VCSEL demonstrate the current confinement effect within the non-implanted area (Fig. 14(a)). Prior to this measurement, the InP/air-gap DBR has been removed. As can be seen, light emission via electron-hole recombination in the active layer occurs only within the non-implanted cylindrical aperture (50 μm diameter) in the center of the photograph. The O^{++} implantation remains thus efficient, even after the thermal annealing of the mid-gap defects during the SS-MBE regrowth (540 °C).

Furthermore, electrical measurements have been carried out on the complete resonant cavity structure including the InP/air-gap mirror. The output signal of these VCSELs under continuous current injection was collected through a microscope objective and fed into an optical spectrometer. The optical spectrum of the device is reported in Fig. 14(b). The F–P peak is clearly

obtained at the resonant wavelength of the cavity. The FHWM of the peak is $\sim$2 nm at 1 $\mathrm{kA/cm^2}$, demonstrating the resonant cavity effect if one compares to the 25 nm wide F–P peak measured from the half-VCSEL chip alone.

However, with increased current, the optical output power tends to saturate and the FWHM of the F–P peak becomes broader, indicating a decrease in the round-trip gain and in cavity finesse, mainly due to heating effects.

6. Conclusion

Different designs for tunable InP-based VCSELs for the 1.55 μm wavelength range have been investigated that are suitable for WDM applications in optical fiber networks. New technologies such as the successful integration of InP/air-gap DBRs and a reliable two chip device technology have been deployed to fabricate photo pumped tunable VCSELs with output powers of as much as 0.5 mW and a maximum tuning range of 24 nm. Furthermore, the monolithic air-gap VCSEL demonstrated the possibility of fabricating very low loss resonators using micromachining technology.

Within the development of an electrically pumped monolithic tunable VCSEL the growth of tunnel junctions by MOVPE has been demonstrated. Good ohmic behavior and low resistance of the tunnel junction diodes have been obtained. The combination of a InGaAlAs/InP DBR with improved thermal conductivity, a MOVPE grown tunnel junction and the established InP/air-gap micromachining technology for a VCSEL structure is the next step.

However, the losses within the microcavity have to be kept as low as possible and the heat dissipation mechanisms need further investigations to improve the performance of the next generation of devices.

Acknowledgements

This work on the design and fabrication of tunable InP-based VCSELs has been done in the framework of the European IST project "TUNVIC" (http://130.83.66.233). Part of this work was supported by the "Région Ile de France" and the "Conseil Général de l'Essonne".

References

[1] T.E. Sale, Vertical-Cavity Surface-Emitting Lasers, Research Studies Press, Taunton, Sommerset, 1985.
[2] H. Li, K. Iga, Vertical Cavity Surface Emitting Laser Devices, in: Springer Ser. Photon., Vol. 6, 2002.
[3] C. Wilmsen, H. Temkin, L. Coldren, Vertical Cavity Surface Emitting Laser Design, Fabrication, Characterization, and Applications, in: Cambridge Stud. Modern Opt., 2002.
[4] F. Koyama, S. Kinoshita, K. Iga, Room-temperature continuous wave lasing characteristics of GaAs vertical cavity surface-emitting laser, Appl. Phys. Lett. 55 (1989) 221–222.
[5] Y.H. Lee, J.L. Jewell, A. Sherer, S.L. McCall, J.P. Harbison, L.T. Florez, Room temperature continuous-wave vertical cavity single quantum well microlaser diodes, Electron. Lett. 25 (1989) 1377–1378.
[6] G.M. Yang, M.H. MacDougal, P.D. Dapkus, Ultralow threshold current vertical cavity surface-emitting lasers obtained with selective oxidation, Electron. Lett. 31 (1995) 886–888.
[7] J.A. Tantun, A. Clark, J.K. Guenter, R.A. Hawthorne, R.H. Johnson, Commercialisation of Honeywell's VCSEL Technology, in: K.D. Choquette, C. Lei (Eds.), Vertical-Cavity Surface Emitting Lasers IV, SPIE–The International Society for Optical Engineering, Proc. SPIE 3946 (2000) 2–13.
[8] S. Rapp, J. Piprek, K. Streubel, J. André, J. Wallin, Temperature sensitivity of 1.54 μm vertical-cavity lasers with an InP-based Bragg reflector, IEEE J. Quantum Electron. 33 (1997) 1839–1845.
[9] K. Kazmierski, J.P. Debray, R. Madani, I. Sagnes, A. Ougazzaden, N. Bouadma, J. Etrillard, F. Alexandre, M. Quillec, +55 °C pulse lasing at 1.56 μm of all-monolithic InGaAlAs-InP vertical cavity lasers, Electron. Lett. 35 (1999) 811–812.
[10] J.K. Kim, E. Hall, O. Sjolmund, G. Almuneau, L.A. Coldren, Room-temperature electrically pumped multiple-active-region VCSELs with high differential efficiency at 1.55 μm, Electron. Lett. 35 (1999) 1084–1085.
[11] O.K. Kwo, B.S. Yoo, J.H. Shin, J.H. Baek, B. Lee, Pulse operation and threshold characteristics of 1.55 μm InGaAlAs-InAlAs VCSELs, IEEE Photon. Technol. Lett. 12 (2000) 1132–1134.
[12] J. Boucart, C. Starck, F. Gaborit, A. Plais, N. Bouché, E. Derouin, J.C. Remy, J. Bonnet-Gamard, L. Goldstein, C. Fortin, D. Carpentier, P. Salet, F. Brillouet, J. Jacquet, Metamorphic DBR and tunnel-junction injection: a CW RT monolithic long-wavelength VCSEL, IEEE J. Selected Topics Quant. Electron. 5 (1999) 520–529.
[13] Y. Ohisho, R. Iga, K. Kishi, C. Amano, Buried heterostructure long-wavelength vertical-cavity surface emitting laser with InGaAsP/InP-GaAs/AlAs DBRs, Electron. Lett. 36 (2000) 3940.
[14] W. Yuen, G.S. Li, R.F. Nabiev, J. Boucart, P. Kner, R.J. Stone, D. Zhang, M. Beaudoin, T. Zheng, C. He, K. Yu, M. Jansen, D.P. Worland, C.J. Chang-Hasnain, High-performance 1.6 μm single-epitaxy step top-emitting VCSEL, Electron. Lett. 36 (2000) 1121–1123.

[15] J.H. Shin, B.S. Yoo, W.S. Han, O.K. Kwon, Y.G. Ju, J.H. Lee, CW Operation and Threshold Characteristcs of All-Monolithic InGaAlAs 1.55 µm VCSELs grown by MOCVD, IEEE Photon. Technol. Lett. 14 (2002) 1031–1033.
[16] M. Ortsiefer, R. Shau, M. Zigldrum, G. Böhm, F. Köhler, M.C. Amann, Submilliamp long-wavelength InP-based vertical-cavity surface-emitting laser with stable linear polarization, Electron. Lett. 36 (2000) 1124–1126.
[17] M.C. Larson, J.S. Harris, Wide and continuous wavelength tuning in a vertical-cavity surface-emitting laser using a micromachined deformable-membrane mirror, Appl. Phys. Lett. 68 (1996) 891–893.
[18] M.S. Wu, E.C. Vail, G.S. Li, W. Yuen, C.J. Chang-Hasnain, Tunable micromachined vertical cavity surface emitting laser, Electron. Lett. 31 (1995) 1671–1672.
[19] M.Y. Li, W. Yuen, G.S. Li, C.J. Chang-Hasnain, Top Emitting micromechanical VCSEL with 31.6 nm tuning range, Photon. Technol. Lett. 10 (1998) 18–20.
[20] M.C. Larson, A.R. Massebgale, J.S. Harris, Continuously tunable micromachined vertical cavity surface emitting laser with 18 nm wavelength range, Electron. Lett. 32 (1996) 330–332.
[21] D. Vakhshoori, P. Tayebati, C.C. Lu, M. Azimi, P. Wang, J.H. Zhou, E. Canoglu, 2 mW CW singlemode operation of a tunable 1550 nm vertical cavity surface emitting laser with 50 nm tuning range, Electron. Lett. 35 (1999) 900–901.
[22] A. Sbyru, V. Iakovlev, G. Suruceanu, C.A. Berseth, A. Rudra, A. Mircea, A. Mereuta, E. Kapon, 1 mW CW 38 nm tunable 1.5 µm VCSELs with tuning voltage below 4 V, in: 28 the European Conf. On Optical Communications, 2002, PD3.8.
[23] C.J. Chang-Hasnain, Tunable VCSEL, J. Select. Topics Quantum Electron. 6 (2000) 978–987.
[24] McLeod, Thin Optical Filters, Adam Hilger, Bristol, 1996.
[25] I. Sagnes, G. Le Roux, C. Mériadec, A. Mereuta, G. Saint-Girons, M. Bensoussan, A new MOCVD InP/AlGaInAs distributed Bragg reflector for 1.55 µm VCSELs, Electron. Lett. 37 (2001) 500–501.
[26] K. Streubel, S. Rapp, J. André, N. Chitica, Fabication of InP/air-gap distributed Bragg reflectors and micro-cavities, J. Math. Sci. Engrg. B 44 (1997) 364–367.
[27] M. Aziz, J. Pfeifer, M. Wohlfarth, S. Wu, P. Meissner, A new and simple concept of tunable two-chip microcavities for filter applications in WDM systems, Photon. Technol. Lett. 12 (2000) 1522–1524.
[28] F. Riemenschneider, M. Aziz, H. Halbritter, I. Sagnes, P. Meissner, Low-cost electrothermally tunable optical microcavities based on GaAs, Photon. Technol. Lett. 14 (2002) 1566–1568.
[29] F. Riemenschneider, I. Sagnes, G. Böhm, H. Halbritter, M. Maute, C. Symonds, M.-C. Amann, P. Meissner, Micro-electro-mechanically tunable two-chip vertical cavity surface emitting laser for long wavelengths, accepted for presentation to European Conference on Lasers and Electro-Optics (CLEO), Munich, Germany, June 2003.
[30] M. Strassner, C. Luber, A. Tarraf, C. Chitica, Widely tunable-constant bandwith monolithic Fabry–Pérot filter with a stable cavity design for WDM systems, IEEE Photon. Technol. Lett. 14 (2002) 1548–1550.
[31] N. Chitica, J. Daleiden, J. Bentell, J. André, M. Strassner, S. Greek, D. Pasquariello, M. Karlsson, R. Gupta, K. Hjort, Fabrication of tunable InP/air-gap Fabry–Pérot cavities by selective etching of InGaAs sacrificial layers, Phys. Scripta 79 (1999) 131–134.
[32] W. Strupinski, M. Czub, J. Gaca, M. Wojcik, Studies on gas-switching sequences influence on the quality of MOVPE InGaAs/InP superlattice structures, in: VII IPRM, Schwäbisch Gmünd, Germany, 1996, pp. 504–506.
[33] M. Strassner, N. Chitica, A. Tarraf, Investigations of growth conditions for InP suited for micro opto electro mechanical systems for data communication, in: XIV IPRM, Stockholm, Sweden, 2002, pp. 351–354.
[34] J.L. Leclercq, P. Regreny, P. Viktorovitch, A. Bakouboula, T. Benyattou, I. Sagnes, G. Saint-Girons, C. Meriadec, A. Mereuta, S. Bouchoule, A. Plais, J. Jacquet, Monolithic tunable InP-based vertical cavity surface emitting laser, DTIP '2002, Proc. SPIE 4755 (2002) 448–454.
[35] E. Hall, S. Nagakawa, G. Almuneau, J.K. Kim, L.A. Coldren, Room-temperature, CW operation of lattice-matched long-wavelength VCSELs, Electron. Lett. 2 (2000) 1465–1467.